Provided for non-commercial research and education use.
Not for reproduction, distribution or commercial use.

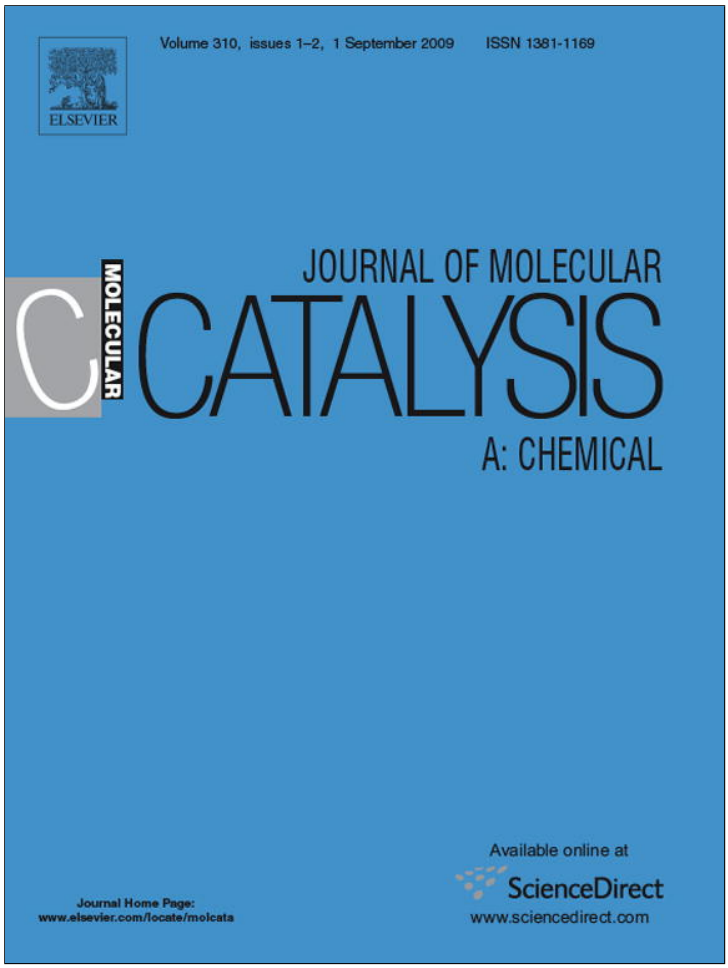

This article appeared in a journal published by Elsevier. The attached copy is furnished to the author for internal non-commercial research and education use, including for instruction at the authors institution and sharing with colleagues.

Other uses, including reproduction and distribution, or selling or licensing copies, or posting to personal, institutional or third party websites are prohibited.

In most cases authors are permitted to post their version of the article (e.g. in Word or Tex form) to their personal website or institutional repository. Authors requiring further information regarding Elsevier's archiving and manuscript policies are encouraged to visit:

http://www.elsevier.com/copyright

Author's personal copy

Journal of Molecular Catalysis A: Chemical 310 (2009) 159–165

Contents lists available at ScienceDirect

Journal of Molecular Catalysis A: Chemical

journal homepage: www.elsevier.com/locate/molcata

Degradation efficiencies and mechanisms of the ZnO-mediated photocatalytic degradation of Basic Blue 11 under visible light irradiation

Chungshin Lu[c], Yingtien Wu[a], Fuder Mai[b], Wenhsin Chung[d], Chiawei Wu[e], Wanyu Lin[d], Chiingchang Chen[a,*]

[a] Department of Science Application and Dissemination, National Taichung University, 140 Ming-Shen Rd., Taichung 403, Taiwan, ROC
[b] Department of Biochemistry, School of Medicine, Taipei Medical University, Taipei 110, Taiwan, ROC
[c] Department of General Education, National Taichung Nursing College, Taichung 403, Taiwan, ROC
[d] Department of Plant Pathology, National Chung Hsing University, Taichung 402, Taiwan, ROC
[e] Department of Applied Chemistry, School of Medicine, Chung-Shan Medical University, Taichung 402, Taiwan, ROC

ARTICLE INFO

Article history:
Received 7 March 2009
Received in revised form 6 June 2009
Accepted 8 June 2009
Available online 17 June 2009

Keywords:
Dye
ZnO
Photocatalytic
Basic Blue 11
HPLC–PDA-MS

ABSTRACT

A ZnO-mediated photocatalysis process was used to successfully degrade Basic Blue 11 (BB-11) under visible light irradiation. The effects of influential factors like initial dye concentration, catalyst dosage, and initial pH were studied. To obtain a better understanding the mechanistic details of ZnO-assisted photodegradation of the BB-11 dye with low watt visible light irradiation, a large number of the intermediates resulting from the photodegradation were separated, identified, and characterized by high-performance liquid chromatography–photodiode array-mass spectrometry (HPLC–PDA-MS) techniques. The results indicated that the *N*-de-alkylation and oxidative degradation of BB-11 dye took place and that *N*-hydroxyalkylated intermediates were generated during the process. From the same identified intermediates we got under UV or visible light irradiation, it is proposed that the major oxidant under visible light irradiation was •OH radical, not $O_2^{-\bullet}$. HPLC–PDA-MS analysis verified the identity of intermediates, and a reaction mechanism based on them was proposed.

© 2009 Elsevier B.V. All rights reserved.

1. Introduction

Triphenylmethane (TPM) dyes have been extensively used as textile dyes for silk, wool, and cotton, in the preparation of inks and in the surface-coating and dyeing of paper, as colorants in cosmetics, drugs, foods, as biological stains, and as anti-infective, antimicrobial, and antihelminthic agents [1,2]. However, the thyroid peroxidase-catalyzed oxidation of the TPM class of dyes has aroused great concern because the reactions might form various *N*-de-alkylated primary and secondary aromatic amines, with structures similar to aromatic amine carcinogens [3–5].

Semiconductor photocatalysts offer huge potential for elimination of toxic chemicals [6]. ZnO, with a wide band gap (3.2 eV), has aroused an explosion of interest in the past few years because of advances in its synthesis and because of its unique optoelectronic, catalytic, and photochemical properties [7–10]. The quantum efficiency of ZnO is also significantly larger than that of TiO_2. In some cases, ZnO has actually proven more effective than TiO_2 [11–13]. The ZnO-mediated photocatalysis process has been successfully used to degrade dye pollutants for the past few years [14–16]. ZnO is available at low cost, which gives it an important advantage. However, the amount of solar UV-light which naturally reaches the earth's surface and is available to excited TiO_2 is relatively small (around 4%) and artificial UV-light sources are somewhat expensive. ZnO's biggest advantage is that it absorbs over a larger fraction of the solar spectrum than TiO_2 [17]. For this reason, ZnO is the most suitable material for photocatalytic degradation in the presence of sunlight. Reports in the literature [17–20] on the photocatalytic degradation of dyes under visible light or sunlight are scare. The effects of various parameters like the initial concentration of substrates, the amount of catalysts, pH values are examined. However, mechanisms of the ZnO-assisted photocatalytic degradation of BB-11 dye under visible light irradiation have not been reported. Therefore, the present work focused on exploring means to effectively utilize visible light sources for treating dye wastewater using ZnO and on the separation and identification of photocatalytic reaction intermediates in hopes of shedding some light on the mechanistic details of the photodegradation of BB-11 dye in the ZnO/vis process. Our results will serve as a foundation for future applications of photocatalytic degradation, solar energy, dye-sensitized photoelectrochemicals, and solid-state solar cells.

* Corresponding author. Tel.: +886 4 2218 3839; fax: +886 4 2218 3530.
E-mail address: ccchen@mail.ntcu.edu.tw (C. Chen).

1381-1169/$ – see front matter © 2009 Elsevier B.V. All rights reserved.
doi:10.1016/j.molcata.2009.06.011

Author's personal copy

2. Experimental

2.1. Chemicals

The ZnO nanoparticle (particle size, ca. 50–70 nm; BET area, ca. 15–25 $m^2\,g^{-1}$) was purchased from Aldrich Chemical Co. The ZnO powder was used as received as a photocatalyst without further purification. P25 TiO_2 was obtained from Degussa and has a surface area of ca. 55 $m^2\,g^{-1}$ and a measured size of the primary particles around 20–30 nm. BB-11 [C.I. 44040] dye was obtained from Sigma–Aldrich and used without any further purification. The chemical structure of this dye is shown in Fig. 1. HPLC analysis was employed to confirm the BB-11 dye as a pure organic compound. 4-(*N*-Methylaminophenol) (**β**; with a guaranteed purity of 98%) and 4-aminoonaphthen-1-ol (**ε**; purity of 90%) were obtained from Aldrich. The 4-(*N*,*N*-methylamino)-4′-(*N*′,*N*′-dmethylamino)benzophenone (**a**) was obtained from Tokyo Kasei Kogyo Co. 4-Aminophenol (**γ**; analytical standard) was purchased from Riedel-de Haen. Reagent-grade ammonium acetate, sodium hydroxide, nitric acid, and HPLC-grade methanol were purchased from Merck. De-ionized water was used throughout this study.

2.2. Apparatus and instruments

The C-75 Chromato-Vue cabinet of UVP provides a wide area of illumination from the 15-W visible light tubes positioned on two sides of the cabinet interior. A Waters ZQ LC/MS system, equipped with a binary pump, a photodiode array (PDA) detector, an autosampler, and a micromass detector, was used for separation and identification. The mineralization of the dye was monitored by measuring the total organic carbon (TOC) content with a Tekmar-Dohrmann Phoenix 8000 TOC Analyzer by directly injecting the aqueous solution.

2.3. Experimental procedures

An aqueous ZnO (or TiO_2) dispersion was prepared by adding ZnO (or TiO_2) powder to a 100 mL solution containing the BB-11 dye at appropriate concentrations. For reactions in different pH media, the initial pH of the suspensions was adjusted by the addition of either NaOH or HNO_3 solutions. Prior to irradiation, the dispersions were magnetically stirred in the dark for ca. 30 min to ensure the establishment of adsorption/desorption equilibrium. Irradiations were carried out using two visible lamps (15 W). At any given irradiation time interval, the dispersion was sampled (5 mL), and centrifuged to separate the ZnO (or TiO_2) particles.

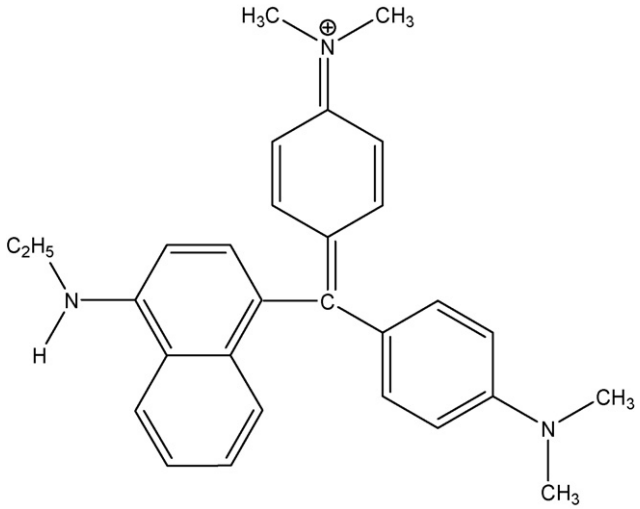

Fig. 1. Chemical structure of BB-11.

2.4. HPLC–PDA–ESI-MS

After each irradiation cycle, the amount of the residual dye was determined by HPLC. The analysis of organic intermediates was accomplished by HPLC–ESI-MS after the readjustment of the chromatographic conditions in order to make the mobile phase compatible with the working conditions of the mass spectrometer. The HPLC gradient program given in Table S1 of Supplementary Materials was used to monitor the intermediates at a flow rate that would accelerate. Intermediates were identified and separated by an Atlantis™ dC18 column (250 mm × 4.6 mm i.d., dp = 5 μm) coupled with a PDA detector selected at λ = 200–700 nm, and the column effluent was introduced into the ESI source of the mass spectrometer.

3. Results and discussion

3.1. Effect of photocatalyst concentration

The effect of photocatalyst concentration on the photodegradation rate of the BB-11 dye was studied by employing different concentrations of ZnO (or TiO_2) ranging from 0.25 to 1.0 g L^{-1}. As expected, the photodegradation rate of the BB-11 was found to increase and then decrease with the increase in the catalyst concentration (Fig. 2). This is a general characteristic of heterogeneous photocatalysts, and our results are in agreement with earlier reports [14]. The results showed that ZnO exhibits higher photocatalytic activity than TiO_2. Above 0.5 g L^{-1} of ZnO, the initial rate of BB-11 degradation is not affected further by a progressive increase in ZnO concentration. This phenomenon may be due to the aggregation of ZnO particles at high concentrations, causing a decrease in the number of surface active sites [12]. However, it is known that there exists a practical limit of the scattering light (around 1 g L^{-1}), above which the degradation rate will decrease due to the reduction of the photonic flux within the irradiated solution [12].

3.2. pH effect

The zero point charge for ZnO is 9.0, and above this value, the ZnO surface is predominantly negatively charged when the pH is higher than the ZnO isoelectric point. Thus, the electrical property of the ZnO surface varies with the pH of the dispersion [21]. Reactions were performed at different pH values using ZnO as a photocatalyst. The role of pH in the photodegradation was studied in the pH

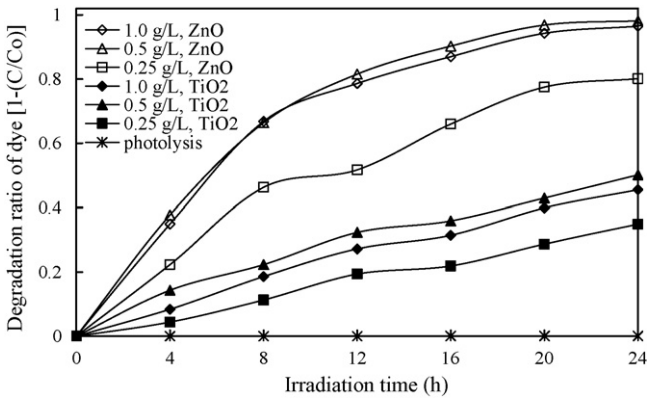

Fig. 2. Influence of the catalyst concentration on the photodegradation rate for the decomposition of BB-11.

Author's personal copy

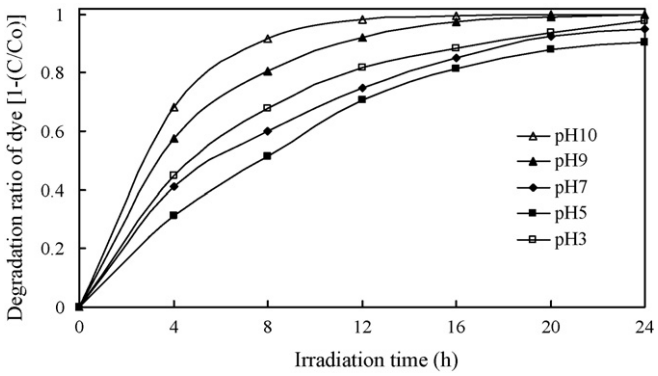

Fig. 3. pH effect on the BB-11 photodegradation rate with concentrations of ZnO to be 0.5 g L^{-1} and BB-11 to be 0.05 g L^{-1}.

range of 3–10 at a 0.05 g L^{-1} dye concentration and 0.5 g L^{-1} catalyst loading. As shown in Fig. 3, the efficiency of the photocatalytic degradation of BB-11 depended on the initial pH of the solution used in the reaction. The photodegradation rate was found to decrease and then increase with increases in pH. At higher pH values, no photocorrosion of ZnO took place. More efficient formation of hydroxyl radical occurred in alkaline conditions. BB-11 has a diethylamino group in its structure which is positively charged; therefore, the dye may be absorbed onto the photocatalyst surface effectively. The formation of active •OH species is favored with higher pH values, due not only to improved transfer of holes to the adsorbed hydroxyls, but also to electrostatic abstractive effects between the negatively charged ZnO particles and the operating cationic dyes. In a good agreement with the adsorption mechanism proposed by Chen [12], the results indicate that the ZnO surface is negatively charged and that the BB-11 was adsorbed onto the ZnO surface through the positive ammonium groups. Although the BB-11 dye can be adsorbed onto the ZnO surface to some extent in alkaline media, the dye molecules will change to a leuco compound when the pH value is too high (pH 11).

On the other hand, a noticeable increase in the photodegradation rate of BB-11 was observed at pH 3. In acidic solutions the photodegradation rate was higher than in neutral solutions. This is because the photodecomposition of ZnO takes place in acid. The photocorrosion of ZnO is complete at pH lower than 4. The formation of Zn^{2+} is attributed to the oxidation of ZnO by h^{+}_{vb} [21–22]. This can be reasonably explained assuming that, at pH 3, ZnO nanoparticle surface is positively charged, thus promoting the migration of photogenerated electrons from the interior of the nanocrystals to the surface and preventing electron–hole recombination processes. It was found to be difficult to adsorb the cationic BB-11 dye onto the ZnO surface under acidic conditions, with active •OH radicals formed at low concentrations, and hence the photodegradation process of BB-11 remained slow. The results show that the photodegradation rate at pH 3 is higher than that at pH 7, but slower than that at pH 9 and 10.

3.3. Effect of dye concentration

In the typical textile effluent, dye concentration ranges from 0.15 to 0.2 g L^{-1}. By varying the initial concentration from 0.05 to 0.2 g L^{-1} at constant catalyst loading (0.5 g L^{-1}, pH 9), its effect on the degradation rate could be determined, and the results are shown in Fig. S1 (Supplementary Materials). As seen in the figure, degradation efficiency is inversely affected by the dye concentration. This negative effect can be explained as follows; as the dye concentration is increased, the equilibrium adsorption of dye on the catalyst surface active sites increases; hence competitive adsorption of O_2 on the same sites decreases, meaning a lower formation rate of $O_2^{-\bullet}$, H_2O_2, and •OH radical, which is the principal oxidant necessary for a high degradation efficiency. On the other hand, considering the Beer-Lambert law, as the initial dye concentration increases, the path length of photons entering the solution decreases, resulting in lower photon adsorption on catalyst particles and, consequently, a lower photodegradation rate.

3.4. Evolution of TOC

The complete mineralization of 1 mol BB-11 dye molecule implies the formation of the equivalent amount (29 mol) of CO_3^{2-} at the end of the treatment. However, the depletion in TOC (Fig. S2 in Supplementary Materials) clearly indicates that the reaction does not go to completion. In fact, after 24 h irradiation, about 76.9% of the initial organic carbon has been transformed into CO_2, which implies that other organic compounds still exist in the irradiated solution. These findings are in agreement with those obtained in a study concerning the photocatalytic degradation of basic violet 4 [23], where the persistence of various aromatic compounds was reported even after long-term irradiation.

3.5. Separation and identification of the intermediates

The chromatogram obtained for an irradiated BB-11 solution after 4 h, at pH 9, with visible light irradiation in the presence of ZnO (0.5 g L^{-1}), and the chromatograms recorded at 580, 350, and 300 nm are illustrated in Fig. S3 of Supplementary Materials. With irradiation up to 20 h, sixty-three components were successfully detected, all with the retention times less than 65 min. We denoted the BB-11 dye and its related intermediates as species **A**–**L**, **A′**–**H′**, **a**–**f**, **a′**–**e′**, **I**–**q**, **I′**–**p′**, **α**–**γ**, **α′**–**β′**, **δ**–**ε** and **δ′**. The maximum absorption band of each intermediate in the visible and ultraviolet spectral region in Tables S2 and 3 of the Supplementary Materials was measured, and they correspond to the peaks in Fig. S3. The intermediates were further identified using the HPLC–ESI mass spectrometric method; the relevant mass spectra are illustrated in Tables S2 and 3. The intermediates appeared to be in acid forms based on their molecular peaks. The concentration of the other intermediates may have been under the detection limit. From these results, intermediates can be classified to several groups.

The first and second groups were signed in the chromatogram and are illustrated in Fig. S3 of Supplementary Materials, recorded at 580 nm. From the results of mass spectral analysis, we confirmed that the component **A**, m/z = 422.69, in the liquid chromatogram is BB-11; the other components are **B**, m/z = 408.20; **C**, m/z = 394.46; **D**, m/z = 394.53; **E**, m/z = 394.45; **F**, m/z = 380.58; **G**, m/z = 380.45; **H**, m/z = 366.43; **I**, m/z = 366.51; **J**, m/z = 366.56; **K**, m/z = 352.61; **L**, m/z = 338.59. The intermediates have the wavelength position of their major absorption bands moved toward the blue region, λ_{max}, **A**, 610.2 nm; **B**, 607.7 nm; **C**, 604.0 nm; **D**, 610.2 nm; **E**, 607.7 nm; **F**, 599.1 nm; **G**, 607.7 nm; **H**, 607.7 nm; **I**, 584.4 nm; **J**, 606.5 nm; **K**, 574.6 nm; **L**, 585.6 nm. The first group of intermediates may represent the *N*-de-alkylation of the BB-11 dye. Mass spectral analysis confirmed the components to be: **A′**, m/z = 438.56; **A″**, m/z = 438.63; **B′**, m/z = 424.74; **B″**, m/z = 424.54; **B‴**, m/z = 424.48; **C′**, m/z = 410.66; **C″**, m/z = 410.53; **D′**, m/z = 410.53; **D″**, m/z = 410.40; **E′**, m/z = 410.62; **F′**, m/z = 396.51; **F″**, m/z = 396.53; **G′**, m/z = 396.45; **G″**, m/z = 396.47; **H′**, m/z = 382.28. The *N*-hydroxyalkylated intermediates (the second group), formed by the hydroxylation of the first group, have the wavelength position of their major absorption band, λ_{max}, **A′**, 604.0 nm; **A″**, 602.8 nm; **B′**, 593.0 nm; **B″**, 604.6 nm; **B‴**, 593.0 nm; **C′**, 583.2 nm; **C″**, 590.5 nm; **D′**, 583.2 nm; **D″**, 597.9 nm; **E′**, 578.3 nm; **F′**, 585.6 nm; **F″**, 612.6 nm; **G′**, 606.5 nm; **G″**, 572.6 nm; **H′**, 605.2 nm; **I′**, 594.2 nm; **J′**, 589.3 nm; **K′**, 584.4 nm.

The third and fourth groups were marked in the chromatogram and are illustrated in Fig. S3, recorded at 350 nm. Mass spectral anal-

Author's personal copy

ysis confirmed the components to be: m/z = 269.09; **b**, m/z = 255.55; **c**, m/z = 241.43; **d**, m/z = 241.36; **e**, m/z = 227.24; **a′**, m/z = 285.13; **b′**, m/z = 271.74. The concentration of the other intermediates may have been under the detection limit. The maximum absorption band of each intermediate in the ultraviolet spectral region around 350 nm is displayed in Table S3, and they correspond to the peaks a–f and a′–e′ in Fig. S3. The **a**–**f** intermediates, produced by the stepwise cleavage of the BB-11 derivatives of the chromophore ring structure or the *N*-de-ethylated **a**, have the wavelength position of their major absorption bands moved toward the blue region, λ_{max}, **a**, 374.0 nm; **b**, 367.9 nm; **c**, 361.2 nm; **d**, 362.1 nm; **e**, 358.1 nm; **f**, 356.2 nm. The intermediates identified in this study, **a**–**f**, were also identified in a previous study of the MG/TiO_2 system [24]. The hydroxylated intermediates (the fourth group, **a′**–**e′**), produced by the hydroxylation of the **a**–**e** intermediates (the third group) or cleavage of the chromophore ring structure of **A′**–**H′** (the second group), have the wavelength position of their major absorption band moved toward the blue region, λ_{max}, **a′**, 359.1 nm; **b′**, 367.9 nm; **b″**, 356.2 nm; **c′**, 361.2 nm; **d′**, 359.1 nm; **e′**, 356.2 nm. The proposed intermediate (**a**) has been compared with standard material of 4-(*N*,*N*-dimethylamino)-4′-(*N*′,*N*′-dimethylamino)benzophenone. The retention times and absorption spectra are identical.

The fifth and sixth groups were marked in the chromatogram and are illustrated in Fig. S3, recorded at 350 nm. Mass spectral analysis confirmed the components to be: **l**, m/z = 319.13; **m**, m/z = 305.29; **l′**, m/z = 335.13; **m′**, m/z = 321.05. The concentration of the other intermediates may have been under the detection limit. The maximum absorption band of each intermediate in the

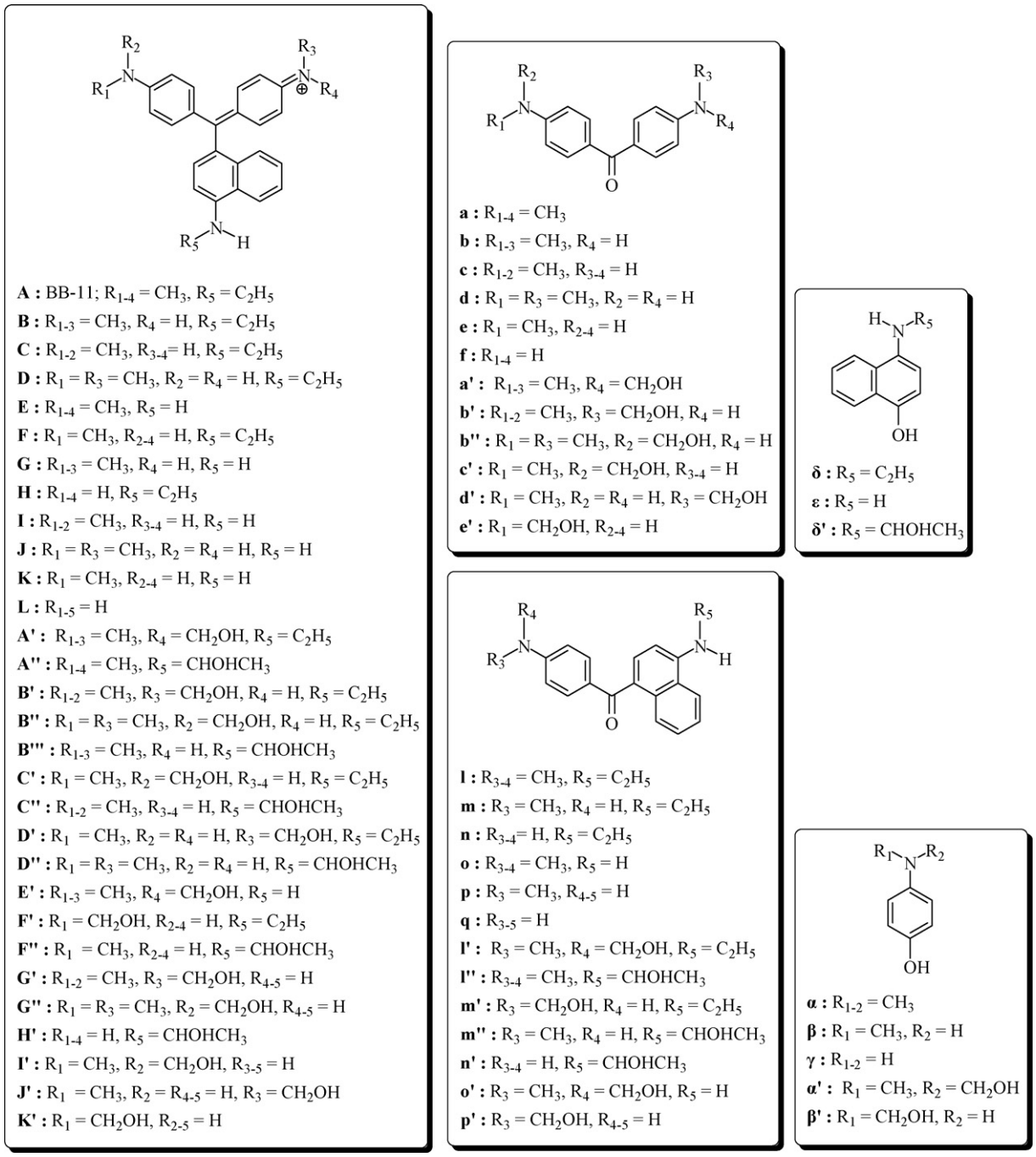

Fig. 4. Chemical structure of photodecomposed intermediates.

Author's personal copy

ultraviolet spectral region around 350 nm is shown in Table S3, and they correspond to the peaks l–q and l′–p′ in Fig. S3. The **l–q** intermediates, produced by cleavage of the chromophore ring structure of **A–L** intermediates (the first group), has the wavelength position of their major absorption bands moved toward the blue region, λ_{max}, **l**, 381.2 nm; **m**, 377.6 nm; **n**, 384.8 nm; **o**, 357.2 nm; **p**, 337.0 nm; **q**, 351.4 nm. The **l′–p′** intermediates, produced by cleavage of the chromophore ring structure of **A′–H′** (the second group) or by hydroxylation of **l–p** intermediates (the fifth group), has the wavelength position of their major absorption bands moved toward the blue region, λ_{max}, **l′**, 347.8 nm; **l″**, 365.5 nm; **m′**, 360.1 nm; **m″**, 355.0 nm; **n′**, 353.8 nm; **o′**, 355.0 nm; **p′**, 345.4 nm.

The seventh and eighth groups were marked in the chromatogram and are illustrated in Fig. S3, recorded at 300 nm. Mass spectral analysis confirmed the components to be: **α**, m/z = 138.24; **δ**, m/z = 188.74. The concentration of the other intermediates may have been under the detection limit. The maximum absorption band of each intermediate in the ultraviolet spectral region around 300 nm is shown in Table S3, and they correspond to the peaks α–γ and δ–ε in Fig. S3. The two group's intermediates, produced

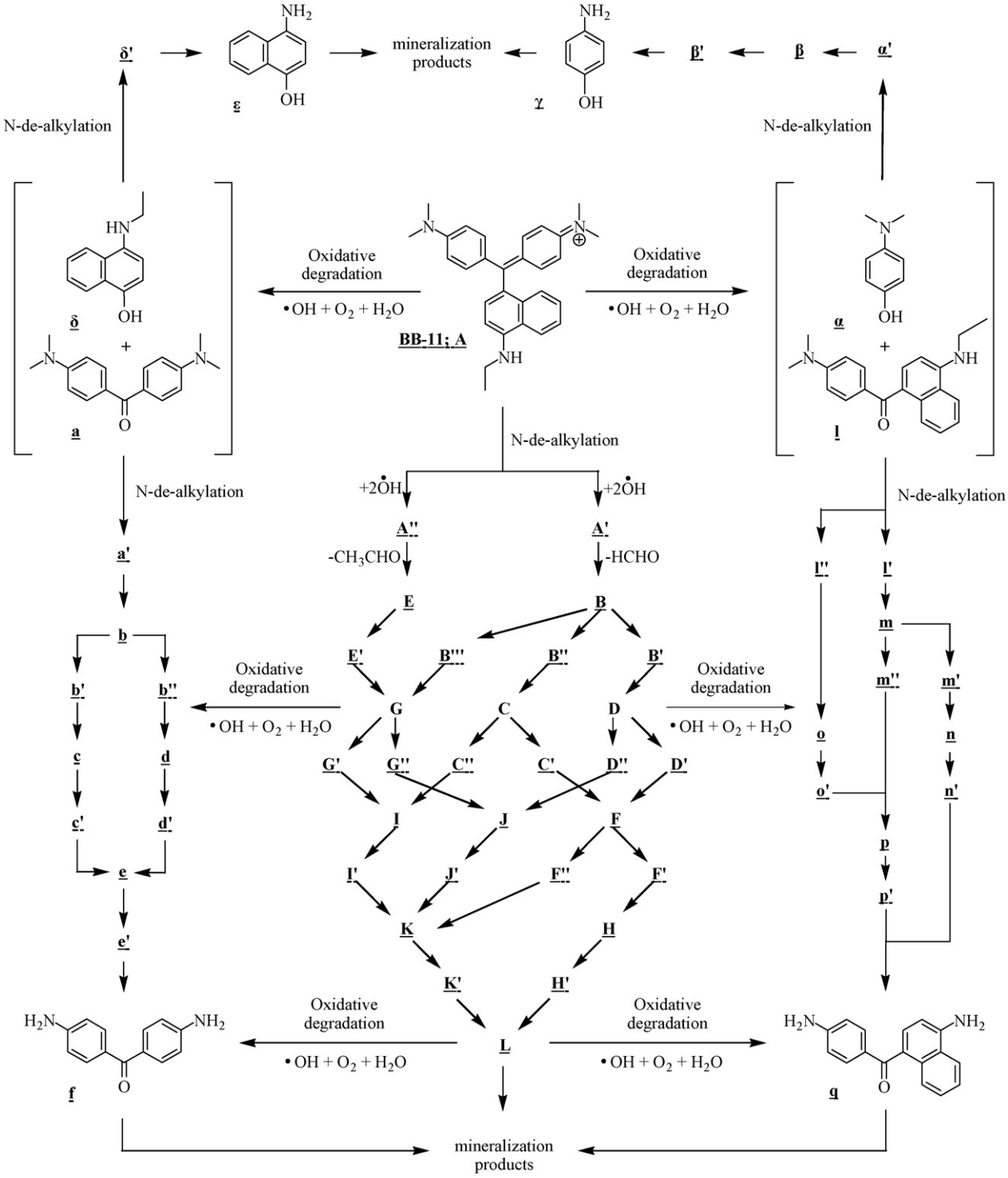

Scheme 1. Proposed mechanisms based on identification of intermediates formed chronologically during the photodegradation of BB-11 dye by HPLC–PDA-MS.

Author's personal copy

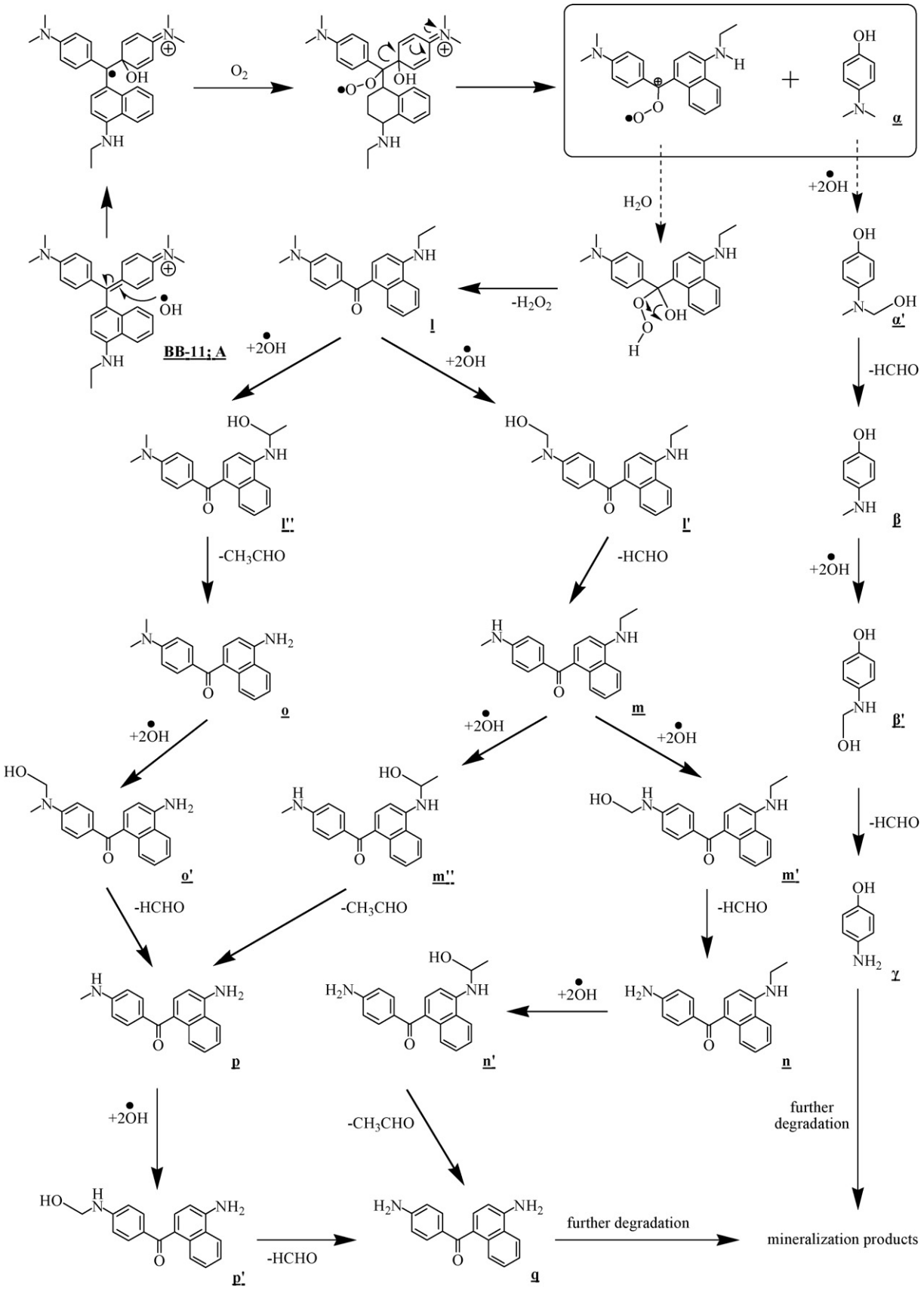

Scheme 2. Proposed oxidation pathway of the BB-11.

Author's personal copy

by cleavage of the first group's intermediates, has the wavelength position of their major absorption bands moved toward the blue region, λ_{max}, **α**, 265.5 nm; **α′**, 271.2 nm; **β**, 244.1 nm; **β′**, 245.3 nm; **γ**, 227.6 nm; **δ**, 286.9 nm; **δ′**, 289.2 nm; **ε**, 279.7 nm. The intermediates identified in this study, **α**–**γ**, were also identified in a previous study of the MG/TiO_2 system [24]. The proposed intermediates (**β**, **γ**, **ε**) have been compared with standard materials of 4-(*N*-dimethylamino)phenol, 4-aminophenol, and 4-aminonaphthen-1-ol. The retention times and absorption spectra are identical. The results we observed above can be seen more clearly in Tables S2 and 3 and chemical structure of intermediates has been shown in Fig. 4.

3.6. Degradation mechanisms of BB-11

Scheme 1 shows the proposed reaction mechanism for the photocatalytic degradation of BB-11 which may occur via two competing and/or parallel pathways. The first pathway involves a hydroxyl radical attack on the *N*,*N*-alkylamino group of BB-11, resulting in a reactive cationic radical, the subsequent de-alkylation and oxidation of which eventually yield the first and second group intermediates. The second pathway involves a hydroxyl radical attack on the central carbon atom of BB-11, yielding a reactive cationic radical, with a bond between the central carbon atom and the *N*,*N*-dimethylamino phenyl ring that is cleaved to give the two sets of intermediates **α** and **l**, and **δ** and **a**. In addition, these intermediates can further be attacked by hydroxyl radicals, giving a reactive cationic radical which is de-alkylated, resulting in **γ**, **q**, **ε** and **f**. The latter intermediates are further oxidized to form mineralization products. The relative distribution of all of the intermediates obtained is illustrated in Fig. S4. The detailed mechanisms are illustrated in Figs. S5 and S6 of Supplementary Materials and Scheme 2.

In earlier reports [7,23–26], the *N*-de-alkylation processes are preceded by the formation of a nitrogen-centered radical while oxidative degradation (destruction of dye chromophore structures) is preceded by the generation of a carbon-centered radical in the photocatalytic degradation of TPM dye. Consistent with this, degradation of BB-11 must occur via three different pathways (two oxidative degradations and one *N*-de-alkylation) due to formation of different radicals (either a carbon-centered or nitrogen-centered radical). There is no doubt that the •OH attack on the dye yields a dye cationic radical. After this step, the cationic radical $dye^{\bullet+}$ can undergo hydrolysis and/or use various de-protonation pathways, which in turn are determined by the different adsorption modes of BB-11 on the TiO_2 particle surface. Both *N*-de-alkylation and oxidative degradation of the BB-11 dye take place in the presence of ZnO particles. These phenomena have been reported in some recent reports relating to TiO_2-mediated photocatalytic degradation [23].

All the intermediates identified in the study were also identified in a previous study of the BB-11/TiO_2/UV system [13]. Under UV irradiation, the initial step in semiconductor-mediated photocatalysed degradation with light energy greater than the band gap energy of the semiconductor is proposed to involve the generation of a (e^-/h^+) pair leading to the formation of hydroxyl radical (•OH). This radical is the oxidizing species in the photocatalytic oxidation processes [14]. Then, under visible irradiation, early reports depict the absorption of light by the dye molecules [21,27]. The excited dye injects an electron into the conduction band of ZnO, where it is scavenged by O_2 to form $O_2^{-\bullet}$. De-alkylation of BB-11 dye occurs mostly through attack by the active species, which is a perfect nucleophilic reagent, on the *N*-alkyl portion of BB-11. Further, $O_2^{-\bullet}$ subsequently reacts with H_2O to generate •OH radical and the other active radical. The probability for the formation of •OH should be much lower than for that $O_2^{-\bullet}$. The •OH is an extremely strong, non-selective oxidant, which leads to the partial or complete mineralization of several organic chemicals. All the above active radicals drive the photodegradation or mineralization of the dye molecule. Under UV or visible light irradiation, all the intermediates identified in these two studied topics have the same result. There is no doubt that the major oxidant is •OH radical, not $O_2^{-\bullet}$.

4. Conclusions

The results showed that ZnO exhibits higher photocatalytic activity than TiO_2 under visible light irradiation. The photodegradation rate of the BB-11 dye was found to increase then decrease along with an increase in the catalyst concentration. This is characteristic of heterogeneous photocatalysts. The efficiency of BB-11 dye photodegradation was found to decrease then increase with an increase in the value of pH. Under visible irradiation, the probability for the formation of •OH should be much lower than for $O_2^{-}\bullet$. Furthermore $O_2^{-\bullet}$ subsequently reacts with H_2O to generate •OH radical oxidant. Because the same identified intermediates were obtained under UV and visible light irradiation, there is no doubt that the major oxidant under visible light irradiation is •OH radical, not $O_2^{-\bullet}$. Both the *N*-de-ethylation and oxidative degradation of BB-11 take place in the presence of ZnO particles with visible light irradiation. The reaction mechanisms of ZnO/vis proposed in this study should shed some light on future applications.

Acknowledgement

This research was supported by the National Science Council of the Republic of China (NSC 97-2113-M-438-002-MY2).

Appendix A. Supplementary data

Supplementary data associated with this article can be found, in the online version, at doi:10.1016/j.molcata.2009.06.011.

References

[1] M.A. Fox, D.F. Duxbury, Chem. Rev. 93 (1993) 381.
[2] Ullmann's Encyclopedia of Industrial Chemistry, Part A27. Triarylmethane and Diarylmethane Dyes, 6th ed., Wiley–VCH, New York, 2001.
[3] B.P. Cho, T. Yang, L.R. Blankenship, J.D. Moody, M. Churchwell, F.A. Bebland, S.J. Culp, Chem. Res. Toxicol. 16 (2003) 285.
[4] S.J. Culp, P.W. Mellick, R.W. Trotter, K.J. Greenlees, R.L. Kodell, F.A. Beland, Food Chem. Toxicol. 44 (2006) 1204.
[5] B.P. Cho, L.R. Blankenship, J.D. Moody, D.R. Doerge, F.A. Beland, S.J. Culp, Tetrahedron 56 (2000) 7379.
[6] M.R. Hoffman, S.T. Martin, W. Choi, W. Bahnemann, Chem. Rev. 95 (1995) 69.
[7] C.C. Chen, C.S. Lu, Environ. Sci. Technol. 41 (2007) 4389.
[8] K. Westermark, H. Rensmo, H.S.K. Keis, A. Hagfeldt, L. Ojameauml, P. Persson, J. Phys. Chem. B 106 (2002) 10102.
[9] L. Bahadur, P. Srivastava, Sol. Energy Mater. Sol. Cells 79 (2003) 235.
[10] T.J. Kuo, C.N. Lin, C.L. Kuo, M.H. Hung, Chem. Mater. 19 (2007) 5143.
[11] V. Kandavelu, H. Kastien, K.R. Thampi, Appl. Catal. B: Environ. 48 (2004) 101.
[12] C.C. Chen, J. Mol. Catal. A: Chem. 264 (2006) 82.
[13] F.D. Mai, C.S. Lu, C.W. Wu, C.H. Huang, J.Y. Chen, C.C. Chen, Sep. Purif. Technol. 62 (2008) 423.
[14] A.H. Akyol, C. Yatmaz, M. Bayramoblu, Appl. Catal. B: Environ. 54 (2004) 19.
[15] M.J. Height, S.E. Pratsinis, O. Mekasuwandumrong, P. Praserthdam, Appl. Catal. B: Environ. 63 (2006) 305.
[16] K. Mehrotra, G.S. Yablonsky, A.K. Ray, Ind. Eng. Chem. Res. 42 (2003) 2273.
[17] I. Poulios, I. Tsachpinis, J. Chem. Technol. Biotechnol. 74 (1999) 349.
[18] B. Parea, S.B. Jonnalagaddab, H. Tomara, P. Singha, V.W. Bhagwata, Desal. 232 (2008) 80.
[19] P.V. Kamat, R. Huehn, R. Nicolaescu, J. Phys. Chem. 106 (2002) 788.
[20] F.D. Mai, C.C. Chen, J.L. Chen, S.C. Liu, J. Chromatogr. A 1189 (2008) 355.
[21] N. Daneshvar, D. Salari, A.R. Khataee, J. Photochem. Photobiol. A: Chem. 162 (2004) 317.
[22] S. Abbruzzetti, M. Carcelli, P. Pelagatti, D. Rominga, C. Viappiani, Chem. Phys. Lett. 344 (2001) 387.
[23] C. Chen, C. Lu, J. Phys. Chem. C 111 (2007) 13922.
[24] J. Lee, W. Choi, Environ. Sci. Technol. 38 (2004) 4026.
[25] C.C. Chen, H.J. Fan, J.L. Jan, J. Phys. Chem. C 112 (2008) 11962.
[26] H. Fu, S. Zhang, T. Xu, Y. Zhu, J. Chen, Environ. Sci. Technol. 42 (2008) 2085.
[27] S. Sun, W. Wang, L. Zhang, L. Zhou, W. Yin, M. Shang, Environ. Sci. Technol. 43 (2009) 2005.